8986 *Inorg. Chem.* **2010**, *49*, 8986–8996
DOI: 10.1021/ic101322s

Inorganic Chemistry
Article

Theoretical and Experimental Study of the Effectiveness of the 5-Pyrimidyl-tetrazolate Bridging Ligand in Mediating Magnetic Exchange Interactions

Antonio J. Mota,[†] A. Rodríguez-Diéguez,[†] M. A. Palacios,[†] J. M. Herrera,[†] Dominique Luneau,[‡] and Enrique Colacio*,[†]

[†]*Departamento de Química Inorgánica, Facultad de Ciencias, Universidad de Granada, Av. Fuentenueva S/N, 18071 Granada, Spain, and* [‡]*Laboratoire des Multimateriaux et Interfaces, Université Claude Bernard, Lyon I, 69622, Villerbanne, France*

Received July 2, 2010

The 5-pyrimidyl-tetrazolate anion (pmtz) has six basic nitrogen atoms and, consequently, can exhibit a variety of bridging coordination modes. This ligand reacts with either copper(II) and nickel(II) ions in the presence of bi- and tridentate amines to afford the following pmtz-bridged complexes: $[Cu_4(\mu\text{-pmtz})_4(tmda)_4](ClO_4)_4$ (**1**) (tmda = *N,N,N′,N′*-tetramethylethylenediamine), $[Cu_2(\mu\text{-pmtz})(tren)_2](ClO_4)_3$ (**2**) (tren = tris(2-aminoethyl)amine), $[Ni_2(\mu\text{-pmtz})(tren)_2](ClO_4)_3$ (**3**), and $[Ni_2(\mu\text{-pmtz})_2(ampa)_2]_n(SCN)_{2n}$ (ampa = bis(3-aminopropyl)amine) (**4**). The structure and bridging coordination mode of these complexes depend on the stereoelectronic preferences of the metal ion and the coordination properties of the polyamine (denticity and relative disposition of the donor atoms). Thus, complex **1** is a square tetranuclear compound where the ligand adopts an asymmetric $k^2N_1,N_7{:}k^2N_4,N_{11}$ bis(chelating)/bridging mode. Complexes **2** and **3** are dinuclear species. In the former the pmtz exhibits a novel $k\text{-}N_1{:}k\text{-}N_4$ imidazolyl/bridging mode whereas the latter shows a symmetric $k^2N_1,N_7{:}k^2N_4,N_{11}$ bis(chelating)/bridging mode. Complex **4** exhibits, however, a linear chain structure where the pmtz ligand connects neighboring nickel(II) atoms by using a tridentate $k^2N_1,N_7{:}kN_3$ chelating/bridging mode. Variable-temperature magnetic susceptibility studies reveal that complexes **1**−**4** show weak to moderate antiferromagnetic (AF) coupling between the metal ions through the pmtz ligand with $J = -14.1\ \text{cm}^{-1}$ for **1**, $J = -31.1\ \text{cm}^{-1}$ for **2**, $J = -4.09\ \text{cm}^{-1}$ for **3**, and $J = -8.7\ \text{cm}^{-1}$ for **4**. The magneto-structural results, as well as DFT theoretical calculations carried out on the experimental geometries and model complexes, demonstrate, first, that the magnitude of the AF interaction observed for imidazolyl pmtz-bridged complexes mainly depends on the Cu−N−C angle (the greater the Cu−N−C angle, the stronger is the AF interaction) and, second, that the tridentate chelating/bridging mode is more effective in mediating AF exchange interactions than the bis(chelating)/bridging or imidazolyl/bridging modes in pmtz-bridged complexes.

Introduction

The chemistry of coordination complexes containing tetrazolate-derived ligands has received a great deal of attention during the past few years.[1] The interest in this kind of complexes is due not only to the rich variety of fascinating structures they can exhibit, which range from zero- to three-dimensional systems, but also to their involvement in areas such as photoluminescence, hydrogen storage, energetic applications, molecular magnetism, and so forth.[1] The 5-pyrimidyl-tetrazolate anion (hereafter pmtz, see Scheme 1) is a versatile ligand that has six basic nitrogen atoms (two on the pyrimidine ring and four on the tetrazolato ring), and consequently exhibits a wide diversity of coordination modes, some of which allow the formation of multidimensional coordination compounds with interesting magnetic,[2] zeolitic,[3] and photoluminescence properties.[4]

Scheme 1. 5-Pyrimidyl-tetrazolate Anion (pmtz) and Its Ring-Numbering System

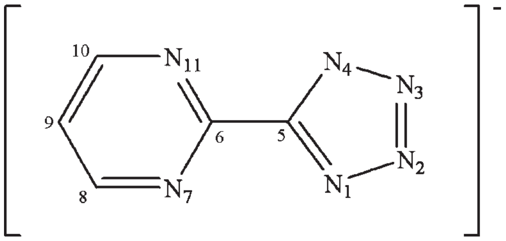

Only a few polynuclear complexes containing paramagnetic transition metal ions and the pmtz bridging ligand have been reported so far.[2] In all cases, pmtz has been shown to be able to mediate antiferromagnetic (AF) interactions between transitions metal ions that, in some cases, lead to bulk magnetic ordering (homometallic and heterometallic spin canted antiferromagnets[2a,c] and ferrimagnets[2b]). It should be noted

---

*To whom correspondence should be addressed. E-mail: ecolacio@ugr.es.

that in none of these cases could the magnitude of the magnetic exchange interaction between the metal ions be determined. In view of this, we decided to prepare relatively simple pmtz-bridged polynuclear copper(II) and nickel(II) complexes with the aim of determining how efficient different bridging coordination modes of the pmtz ligand are in mediating AF interactions. The knowledge of this would be very useful for designing magnetically interesting pmtz-containing materials. To get compounds with different pmtz-bridging coordination modes we have used polyamines as coligands (see below), which exhibit different coordinative properties (number and disposition of the nitrogen donor set). We report below the synthesis, crystal structures, magnetic properties, and density functional theory (DFT) calculations of four new polynuclear complexes bearing the pmtz-bridging ligand: $[Cu_4(\mu\text{-pmtz})_4(tmda)_4](ClO_4)_4$ (**1**) (tmda = *N,N,N′,N′*-tetramethylethylenediamine), $[Cu_2(\mu\text{-pmtz})(tren)_2](ClO_4)_3$ (**2**) (tren = tris(2-aminoethyl)amine), $[Ni_2(\mu\text{-pmtz})(tren)_2](ClO_4)_3$ (**3**), and $[Ni_2(\mu\text{-pmtz})_2(ampa)_2]_n(SCN)_{2n}$ (ampa = bis(3-aminopropyl)amine) (**4**).

Experimental Section

General Procedures. All analytical reagents were purchased from commercial sources and used without further purification. The sodium salt of the pmtz ligand was prepared according to a previously described procedure.[2c]

Preparation of the Complexes. $Cu_4(\mu\text{-pmtz})_4(tmda)_4](ClO_4)_4\cdot 16H_2O$ (1). To a solution of $Na(pmtz)\cdot(H_2O)$ (0.103 g, 0.588 mmol) in 20 mL of water were successively added tmda (0.089 mL, 0.588 mmol) and $Cu(ClO_4)_2\cdot 6H_2O$ (0.218 g, 0.588 mmol) in methanol (10 mL), and the mixture was stirred for 30 min. After filtering a violet precipitate corresponding to the complex $[Cu(tmda)_2(ClO_4)_2]$, the blue filtrate solution was kept at room temperature. X-ray quality blue crystals of **1**, together with violet crystals of $[Cu(tmda)_2(ClO_4)_2]$, were obtained by slow evaporation of the solution after several days. Crystals of **1** were manually separated and air-dried. Yield: 10%. Anal. Calcd for $C_{44}H_{108}Cl_4Cu_4O_{32}$: C, 26.51; H, 5.46; N, 22.48. Found: C, 26.69; H, 5.41; N, 22.16; IR (KBr, cm^{-1}): 3448 ν (OH); 1578, ν (C=C); 1473, 1398, ν (CN): 1094 ν (ClO_4).

$[Cu_2(tren)_2(\mu\text{-pmtz})(ClO_4)_3]$ (2). To a solution of $Na(pmtz)\cdot(H_2O)$ (0.103 g. 0.588 mmol) in 20 mL of H_2O was slowly added a solution of $Cu(ClO_4)_2.6H_2O$ (0.436 g, 1.176 mmol) in 20 mL of acetonitrile containing tris(2-aminoethyl)amine (0.177 mL, 1.176 mmol). After stirring the solution for 30 min at 50 °C a blue precipitate appeared, which was filtered-off and recrystallized in a methanol/water mixture 2:1 v/v. The resulting blue solution was left standing at room temperature for 2 days. Blue crystals of **2** formed, which were filtered off and air-dried. Yield: 70%. Anal. Calcd for $C_{17}H_{35}Cl_3N_{14}Cu_2O_{12}$: C, 23.60; H, 4.54; N, 22.67. Found: C, 23.42; H, 4.68; N, 22.49. IR (KBr, cm^{-1}): 3355 ν_{as} (NH_2); 3305 ν_{sym} (NH_2); 3090 ν $(C-H)_{pym}$; 1594, ν (C=C); 1472 y 1406, ν (CN): 1087 ν (ClO_4).

$[Ni_2(\mu\text{-pmtz})(tren)_2](ClO_4)_3\cdot H_2O$ (3). A solution of $Ni(ClO_4)_2\cdot 6H_2O$ (0.43 g, 1.176 mmol) and tren (0.176 mL, 1.176 mmol) in 40 mL of methanol was added to a solution of $Na(pmtz)\cdot(H_2O)$ (0.103 g, 0.588 mmol) in 10 mL of water. The mixture was stirred at 50 °C for 30 min and then filtered to remove any amount of a light violet solid that corresponds to the complex $[Ni(tren)(ClO_4)]ClO_4$. The violet filtrate was allowed to stand at room temperature for several days, affording light violet crystals of **2**. Yield: 20% Anal. Calcd for $C_{17}H_{41}Cl_3N_{14}Ni_2O_{13}$: C, 23.38; N, 22.45; H 4.73. Found: C, 23.52; N, 22.14; H, 5.10. IR (KBr, cm^{-1}): 3339 ν_{as} (NH_2); 3293 ν_{sym} (NH_2); 3092 ν $(C-H)_{pym}$; 1587, ν (C=C); 1481 y 1406, ν (CN): 1081 ν (ClO_4).

$[Ni_2(\mu\text{-pmtz})_2(ampa)_2]_n(SCN)_{2n}$ (4). To a stirred solution of $Ni(NO_3)_2\cdot 6H_2O$ (0.291 g, 1.0 mmol) in methanol (30 mL) was added *N*-(3-aminopropyl)-1,3-propanediamine (141 μL, 1.0 mmol), and the mixture was kept at room temperature for 5 min. Then, $Na(pmtz)\cdot(H_2O)$ (0.176 g, 1.0 mmol) in water (5 mL) and KSCN (0.097 g, 1.0 mmol) in water (5 mL) were successively added to the blue solution. The mixture was heated at 60° for 30 min, and it then was cooled down at room temperature. The blue solution was filtered off, and the filtrate was left to evaporate at room temperature, yielding blue-purple crystals of **4** (312 mg, 74.6%) that were collected by filtration and air-dried. Yield: 75% Anal. Calcd for $C_{24}H_{40}N_{20}Ni_2\ S_2$: C, 36.48; N, 35.45; H 5.10; S, 8.11. Found: C, 36.45; N, 35.29; H, 5.30; S, 8.21. IR (KBr, cm^{-1}): 3299 ν_{as} (NH_2); 3237 ν_{sym} (NH_2); 3091 ν $(C-H)_{pym}$; 2052 ν (SCN); 1584, ν (C=C); 1455; ν (CN): 1081 ν (ClO_4).

Computational Details. All theoretical calculations were carried out at the DFT level of theory using the hybrid B3LYP exchange-correlation functional,[5] as implemented in the Gaussian 03 program.[6] A quadratic convergence method was employed in

---

(1) (a) Tao, J.; Ma, Z. J.; Huang, R. B.; Zheng, L. S. *Inorg. Chem.* **2004**, *43*, 6133. (b) Jiang, C.; Yu, Z. P.; Wang, S.; Jiao, C.; Li, J. M.; Wang, Z. Y.; Cui, Y. *Eur. J. Inorg. Chem.* **2004**, 3662. (c) Xiong, R. G.; Xue, X.; Zhao, H.; You, X. Z.; Abrahams, B. F.; Xue, Z. *Angew. Chem., Int. Ed.* **2002**, *41*, 3800. (d) Wang, L. Z.; Qu, Z. R.; Zhao, H.; Wang, X.-S.; Xiong, X.-G.; Xue, Z.-L. *Inorg. Chem.* **2003**, *42*, 3969. (e) Mautner, F. A.; Gspan, C.; Gatterer, K.; Goher, M. A. S.; Abu-Youssef, A. M.; Bucher, E.; Sitte, W. *Polyhedron* **2004**, *23*, 1217. (f) Jiang, C.; Mo, X.-J.; Gao, E.-Q.; He, Z.; Li, W. J.; Yan, C. H. *Inorg. Chem. Commun.* **2004**, *7*, 353. (g) Wu, T.; Yi, B.-H.; Li, D. *Inorg. Chem.* **2005**, *44*, 4130. (h) Luo, T.-T.; Tsai, H.-L.; Yang, S. L.; Liu, Y. H.; Yadav, R. D.; Su, C.-C.; Ueng, C.-H.; Lin, L.-G.; Lu, K.-L. *Angew. Chem., Int. Ed.* **2005**, *44*, 6063. (i) Lin, P.; Clegg, W.; Harrington, R. W.; Henderson, R. A. *Dalton Trans.* **2005**, 2388. (j) Wu, T.; Chen, M.; Li, D. *Eur. J. Inorg. Chem.* **2006**, 2132. (k) Wu, T.; Zhou, R.; Li, D. *Inorg. Chem. Commun.* **2006**, *9*, 341. (l) He, X.; Lu, C.-Z.; Yuan, D.-Q. *Inorg. Chem.* **2006**, *45*, 5760. (m) Zhang, X.-M.; Zhao, Y.-F.; Wu, H.-S.; Batten, S. R.; Ning, S. W. *Dalton Trans.* **2006**, 3170. (n) Abu-Youssef, M. A. M.; Mautner, F. A.; Massoud, A. A.; Oehrstroem, L. *Polyhedron* **2007**, *26*, 1531. (o) Luo, J.; Zhang, X.-R.; Cui, L.-L.; Dai, W.-Q.; Liu, B.-S. *Acta Crystallogr.* **2006**, *C62*, m614. (p) Zhang, X.-L.; Zhang, C. L.; Qiu, Y. E.; An, N. *Acta Crystallogr.* **2007**, *E63*, m2423. (q) Fan, S. D.; Liu, J. T. *Acta Crystallogr.* **2007**, *E63*, m2034. (r) Liu, J. T.; Fan, S. D. *Acta Crystallogr.* **2007**, *E63*, m1942. (s) Liu, J. T.; Fan, S. D. *Acta Crystallogr.* **2007**, *E63*, m1652. (t) Rodríguez-Diéguez, A.; Colacio, E. *Chem. Commun.* **2006**, 4140. (u) Dinca, M.; Yu, A. F.; Long, J. R. *J. Am. Chem. Soc.* **2006**, *128*, 8904. (v) Dinca, M.; Long, J. R. *J. Am. Chem. Soc.* **2007**, *129*, 11172. (w) Dinca, M.; Han, W. S.; Liu, Y.; Dailly, A.; Brown, C. M.; Long, J. R. *Angew. Chem., Int. Ed.* **2007**, *46*, 1419. (x) Dinca, M.; Dailly, A.; Liu, Y.; Brown, C. M.; Neumann, D. A.; Long, J. R. *J. Am. Chem. Soc.* **2006**, *128*, 16876. (y) Li, Z.; Li, M.; Zhou, X.-P.; Wu, T.; Ning, S. W. *Cryst. Growth Des.* **2007**, *7*, 1992. (z) Qiu, Y.-E *Acta Crystallogr.* **2007**, *E63*, m2872. (aa) Liu, J.-T.; Fan, S.-D. *Acta Crystallogr.* **2007**, *E63*, m1632. (ab) Jin, M.-F.; Qiu, Y.-E.; Zhang, X.-L. *Acta Crystallogr.* **2007**, *E63*, m2718. (ac) Klapötke, T. M.; Sabaté, C. M.; Rasp, M. *Dalton Trans.* **2009**, 1825.

(2) (a) Rodríguez, A.; Kivekäs, R.; Colacio, E. *Chem. Commun.* **2005**, 5228. (b) Li, J.-R.; Yu, Q.; Sañudo, C. E.; Tao, Y.; Song, W.-C.; Bu, X.-H. *Chem. Mater.* **2008**, *20*, 1218. (c) Rodríguez-Diéguez, A.; Palacios, M. A.; Sironi, A.; Colacio, E. *Dalton Trans.* **2008**, 2887.

(3) Zhang, J.-Y.; Cheng, A.-L.; Yue, Q.; Sun, W.-W.; Gao, E.-Q. *Chem. Commun.* **2008**, 847.

(4) (a) Rodríguez-Diéguez, A.; Salinas-Castillo, A.; Galli, S.; Masciocchi, N.; Gutiérrez-Zorrilla, J. M.; Vitoria, P.; Colacio, E. *Dalton Trans.* **2007**, 1821. (b) Rodríguez-Diéguez, A.; Mota, A. J.; Seco, J. M.; Palacios, M. A.; Romerosa, A.; Colacio, E. *Dalton Trans.* **2009**, 9578.

(5) (a) Becke, A. D. *Phys. Rev. A* **1988**, *38*, 3098. (b) Lee, C. T.; Yang, W. T.; Parr, R. G. *Phys. Rev. B* **1988**, *37*, 785. (c) Becke, A. D. *J. Chem. Phys.* **1993**, *98*, 5648.

(6) Frisch, M. J.; Trucks, G. W.; Schlegel, H. B.; Scuseria, G. E.; Robb, M. A.; Cheeseman, J. R.; Montgomery, Jr., J. A.; Vreven, T. ; Kudin, K. N.; Burant, J. C.; Millam, J. M.; Iyengar, S. S.; Tomasi, J.; Barone, V.; Mennucci, B.; Cossi, M.; Scalmani, G.; Rega, N.; Petersson, G. A.; Nakatsuji, H.; Hada, M.; Ehara, M.; Toyota, K.; Fukuda, R.; Hasegawa, J.; Ishida, M.; Nakajima, T.; Honda, Y.; Kitao, O.; Nakai, H.; Klene, M.; Li, X.; Knox, J. E.; Hratchian, H. P.; Cross, J. B.; Adamo, C.; Jaramillo, J.; Gomperts, R.; Stratmann, R. E.; Yazyev, O.; Austin, A. J.; Cammi, R.; Pomelli, C.; Ochterski, J. W.; Ayala, P. Y.; Morokuma, K.; Voth, G. A.; Salvador, P.; Dannenberg, J. J.; Zakrzewski, V. G.; Dapprich, S.; Daniels, A. D.; Strain, M. C.; Farkas, O.; Malick, D. K.; Rabuck, A. D.; Raghavachari, R.; Foresman, J. B.; Ortiz, J. V.; Cui, Q.; Baboul, A. G.; Clifford, S.; Cioslowski, J.; Stefanov, B. B.; Liu, G.; Liashenko, A.; Piskorz, P.; Komaromi, I.; Martin, R. L.; Fox, D. J.; Keith, T.; Al-Laham, M. A.; Peng, C. Y.; Nanayakkara, A.; Challacombe, M.; Gill, P. M. W.; Johnson, B.; Chen, W.; Wong, M. W.; Gonzalez, C.; Pople, J. A. *Gaussian 03*, revision C.02; Gaussian, Inc.: Wallingford, CT, 2004.

Table 1. Crystallographic Data and Structural Refinement Details for **1**−**4**

	1	**2**	**3**	**4**
chemical formula	$C_{44}H_{76}N_{32}O_{15.5}C_{14}Cu_4$	$C_{17}H_{39}N_{14}O_{12}C_{13}Cu_2$	$C_{17}H_{39}N_{14}O_{13}C_{13}Ni_2$	$C_{24}H_{40}N_{20}S_2Ni_2$
M/g mol^{-1}	1697.33	865.05	871.39	790.30
T (K)	293	293	293	293
λ/Å	0.71073	0.71073	0.71073	0.71073
cryst syst	monoclinic	tetragonal	orthorhombic	monoclinic
space group	$P21/c$	$P\bar{4}21m$	$P212121$	Cc
a/ Å	17.378(5)	11.914(1)	12.260(5)	23.008(4)
b/ Å	30.343(5)	11.914(1)	16.142(5)	9.016(5)
c/ Å	17.922(5)	12.014(1)	17.471(5)	17.759(5)
α/ deg	90	90	90	90
β/ deg	112.669(5)	90	90	113.55(2)
γ/ deg	90	90	90	90
V/ Å^3	8720(4)	1705.2(2)	3458(2)	3377(2)
Z	4	2	4	4
ρ (g cm^{-3})	1.293	1.685	1.674	1.554
μ (mm^{-1})	1.152	1.557	1.399	1.291
unique reflections	53887	10803	22064	6121
$R(int)$	0.089	0.042	0.052	0.000
GOF on F^2	0.931	1.004	1.010	1.027
R1 [$I > 2\sigma(I)$][a]	0.083	0.041	0.072	0.051
wR2 [$I > 2\sigma(I)$][a]	0.208	0.103	0.175	0.118

[a] $R(F) = \sum||F_o| - |F_c||/\sum|F_o|$, $wR(F^2) = [\sum w(F_o^2 - F_c^2)^2/\sum wF_o^4]^{1/2}$.

the SCF process.[7] Triple-ζ quality basis set proposed by Ahlrichs and co-workers has been used for all atoms.[8] The calculations were performed on the complexes built from the experimental geometries as well as on model complexes.

The electronic configurations used as starting points were created using the Jaguar 7.6 software.[9] The approach that we used herein to determine the exchange coupling constants for polynuclear complexes has been described in detail elsewhere.[10]

Physical Measurements. Elemental analyses were carried out at the "Centro de Instrumentación Científica" (University of Granada) on a Fisons-Carlo Erba analyzer model EA 1108. The IR spectra on powdered samples were recorded with a ThermoNicolet IR200FTIR by using KBr pellets. Magnetization and variable temperature (1.9−300 K) magnetic susceptibility measurements on polycrystalline samples were carried out with a Quantum Design SQUID MPMS XL-5 device operating at different magnetic fields. The experimental susceptibilities were corrected for the diamagnetism of the constituent atoms by using Pascal's tables.

Single-Crystal Structure Determination. Suitable crystals of **1**−**4** were mounted on glass fiber and used for data collection. Data were collected with a Bruker AXS APEX CCD area detector equipped with graphite monochromated Mo Kα radiation ($\lambda = 0.71073$ Å) by applying the ω-scan method. Lorentz-polarization and empirical absorption corrections were applied.[11] The structures were solved by direct methods[12] and refined with full-matrix least-squares calculations on F^2.[13a] Attempts to identify the solvent molecules (water) failed in compound **1**. Instead, a new set of $F^2(hkl)$ values with the contribution from solvent molecules withdrawn was obtained by the SQUEEZE procedure implemented in PLATON_94.[13b] Anisotropic temperature factors were assigned to all atoms except hydrogens, which were made to ride with their parent atoms with an isotropic temperature factor arbitrarily chosen as 1.2 times that of the respective parent. Final $R(F)$, $wR(F^2)$ and goodness of fit agreement factors, details on the data collection and analysis can be found in Table 1. Crystallographic data (excluding structure factors) for the reported structure have been deposited with the Cambridge Crystallographic Data Centre as supplementary publication CCDC No. 780301−780304. Copies of the data can be obtained free of charge upon application to CCDC, 12 Union Road, Cambridge CB2 1EZ, U.K. (fax, (+44)1223 336−033; e-mail, deposit@ ccdc.cam.ac.uk).

Results and Discussion

The use of tmda as a chelating coligand favors the formation of complexes with cyclic and chain structures instead of mononuclear species because the steric hindrance arising from crowding of the methyl groups would prevent the coordination of two tmda ligands to the same copper(II) center in *cis* positions. Thus, the reaction of Napmtz with $Cu(ClO_4)_2 \cdot 6H_2O$ and tmda in 1:1:1 molar ratio, using a water/methanol mixture as solvent, afforded the tetranuclear compound $[Cu_4(\mu\text{-pmtz})_4(tmda)_4](ClO_4)_4$. All attempts to obtain the analogous Ni^{II} complex were unsuccessful. This may be due to the stereochemical rigidity of the Ni(II) coordination sphere compared to the stereochemical plasticity of the Cu(II) ion. When tren is used as coligand (tren blocks four coordination positions on the coordination sphere of the metal ion and leaves, in the case of the copper(II) ion, only one available coordination position), the reaction between Napmtz with $Cu(ClO_4)_2 \cdot 6H_2O$ and tren in 1:1:1 molar ratio led to the mononuclear complex $[Cu(tren)(pmtz)]ClO_4$, where the pmtz ligand is monocoordinated to the copper ion through the N1 tetrazolate nitrogen atom (see Scheme 1 for atom numbering).[4b] However, if a 1:2:2 molar ratio is used [excess of the Cu(tren)$^{2+}$ unit] the dinuclear compound $[Cu_2(pmtz)(tren)_2](ClO_4)_3$ (**2**) is obtained. In this compound

---

(7) Bacskay, G. B. *Chem. Phys.* **1981**, *61*, 385.

(8) Schäfer, A.; Huber, C.; Ahlrichs, R. *J. Chem. Phys.* **1994**, *100*, 5829.

(9) *Jaguar*, version 7.6; Schrödinger, Inc.: Portland, OR, 2009.

(10) (a) Ruiz, E.; Cano, J.; Alvarez, S.; Alemany, P. *J. Comput. Chem.* **1999**, *20*, 1391. (b) Ruiz, E.; Alvarez, S.; Rodríguez-Fortea, A.; Alemany, P.; Puoillon, Y.; Massobrio, C. In *Magnetism: Molecules to Materials*; Miller, J. S., Drillon, M., Eds.; Wiley-VCH: Weinheim, 2001; Vol. *II*, p 5572. (c) Ruiz, E.; Rodríguez-Fortea, A.; Cano, J.; Alvarez, S.; Alemany, P. *J. Comput. Chem.* **2003**, *24*, 982. (d) Ruiz, E.; Alvarez, S.; Cano, J.; Polo, V. *J. Chem. Phys.* **2005**, *123*, 164110.

(11) Sheldrick, G. M. *SADABS, Program for Empirical Absorption Correction*; University of Göttingen: Göttingen, Germany, 1996.

(12) Altomare, A.; Cascarano, G.; Giacovazzo, C.; Guagliardi, A.; Moliterni, A. G. G.; Burla, M. C.; Polidori, G.; Cavalli, M.; Spagna, R. *SIR97: package for structure solution by direct methods*; University of Bari: Bari, Italy, 1997.

(13) (a) Sheldrick, G. M. *SHELX97: program for crystal structure refinement*; University of Göttingen: Göttingen, Germany, 1997. (b) Spek, A. L. *PLATON-94* (*V-101094*), *A Multipurpose Crystallographic Tool*; University of Utrecht: The Netherlands, 1994.

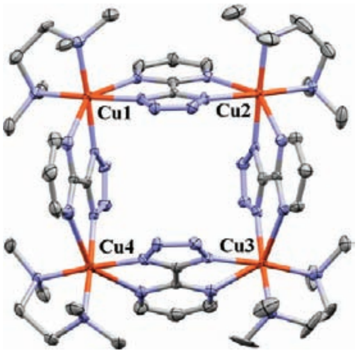

Figure 1. Perspective view of the of the structure of **1**. Thermal ellipsoids are drawn at the 35% probability level. Perchlorate anions and hydrogen atoms are omitted for the sake of clarity.

a bidentate nonchelating bridging mode of the pmtz ligand is expected. The reaction of Napmtz with Ni(ClO$_4$)$_2$·6H$_2$O and tren in 1:2:2 molar ratio led to the expected dinuclear complex [Ni$_2$(pmtz)(tren)$_2$](ClO$_4$)$_3$ (**3**). Because the tren ligand leaves two *cis* available positions on the Ni(II) coordination sphere, a (chelating)/bridging coordination mode is expected for the pmtz ligand in **3**. Finally, by using the ampa coligand, that blocks three positions on the coordination sphere of the Ni(II) ion in a *mer* disposition, the chain complex [Ni$_2$(μ-pmtz)$_2$(ampa)$_2$]$_n$(SCN)$_{2n}$ (**4**) was obtained. Therefore, the number and disposition of the nitrogen donor set of the polyamine has a direct influence on the bridging coordination mode adopted by the pmtz ligand and, consequently, on the final structure of the complex.

Structures. The structure of **1** consists of cationic square [Cu$_4$(μ-pmtz)$_4$(tmda)$_4$]$^{4+}$ units and four perchlorate anions. Within the tetranuclear units (see Figure 1), four crystallographically independent Cu(II) ions are bridged by pmtz ligands exhibiting a novel asymmetric k^2N$_1$,N$_7$:k^2N$_4$,N$_{11}$ bis(chelating)/bridging mode with two long N$_{\mathrm{pym}}$−Cu distances of about 2.7 Å and two short N$_{\mathrm{tetr}}$−Cu distances of about 2.0 Å, pym and tetr subindices referring to the pyrimidine and tetrazolate coordinated nitrogen atoms, respectively. Cu(II) ions exhibit a highly distorted octahedral CuN$_6$ coordination environment. In this description, four short bonds are formed in the equatorial plane with two tetrazolate nitrogen atoms belonging to two different pmtz ligands and two nitrogen atoms from the tmda chelating ligand. In axial positions, at longer distances, are located the pyrimidine nitrogen atoms of two different pmtz ligands. While the *cis* and *trans* angles in the equatorial planes are close to 90° and 180°, the angles involving the axial ligands significantly deviate from these values, with *cis* and *trans* angles in the ranges 70.70°−105.61° and 149.14°−149.88°, respectively. The distortion of the CuN$_6$ octahedron is mainly due to the small bite of the pmtz ligand (about 71°). Tris(bidentate) MN$_6$ units display a propeller-like chirality and, therefore, the copper(II) ions can exhibit a Δ or Λ stereochemistry. Owing to the pseudo-C_{2v} symmetry of the tetranuclear cations (the C_2 axis would be perpendicular to the plane containing the four copper atoms and would pass through the barycenter of the square, whereas the mirror planes would contain the C_2 axis and would pass through the half of opposite pmtz ligands) each metal ion is related to the neighboring ones by mirror planes and, consequently, each pair of neighboring metal ions have opposite chirality. The presence of an inversion center in the lattice generates an equal amount of heterochiral $\Lambda\Delta\Lambda\Delta$ and $\Delta\Lambda\Delta\Lambda$ enantiomers in the crystal, resulting in a racemic structure. The M···M distances across the pmtz ligand and through diagonals are of about 5.9 Å and 8.3 Å, respectively. The tetrazolate rings of the ligands converge alternatively above and below the plane of the square toward the normal to this plane, whereas the pyrimidine groups adopt, in consequence, divergent orientations (see Figure 1). The dihedral angles between the planes of neighboring ligands are close to 84°, whereas the dihedral angles between the plane defined by the copper(II) atoms and the mean planes of the ligands are close to 71°. This disposition of the ligands leads to the formation of a bowl-shaped capsule. Bond distances and angles of the pmtz ligand are similar to those observed in other pmtz-containing complexes.[2−4]

Centrosymmetric related tetranuclear units are disposed in such a way that square channels of about 3.5 Å × 3.5 Å are formed along the *c* axis (see Figure 2).

The structure of **2** is made of dinuclear [Cu$_2$(μ-pmtz)(tren)$_2$]$^{3+}$ cations with C_{2v} symmetry and three perchlorate anions (Figure 3). The copper(II) ions in the dinuclear cation are bridged by a pmtz ligand acting in a novel symmetric k-N$_1$:k-N$_4$ imidazolyl bridging mode similar to that observed in **1** if the long axial interactions are not taken into account. Because of the C_{2v} symmetry, both halves of the dinuclear cationic unit are symmetrically related by a 2-fold axis and two mirror planes, one of them containing the pmtz ligand and the other one perpendicular to this and passing through the barycenter of the pyrimidine and tetrazolate rings. The 2-fold axis is found at the intersection of the two mirror planes. Copper(II) atoms exhibit a CuN$_5$ coordination environment with a distorted trigonal-bipyramid geometry (τ = 0.63, τ being 1 for a trigonal bipyramid geometry and 0 for a square-pyramid geometry). In this description, each of the symmetry-related N1 and N4 atoms (N1A and N1A′ in Figure 3) belonging to the pmtz bridging ligand occupy one of the axial positions on their respective coordination polyhedra. Cu−N bond distances are in the range 1.990(3)−2.151(5) Å, the shorter one corresponding to the Cu−N$_{\mathrm{tetr}}$ bond distance and the longer one to one of the Cu−N$_{\mathrm{tren}}$ bond distances. The C−N−Cu bond angle at the tetrazolate bridging region is 130.53(3)°, which is rather larger than those observed in **1**.

The structure of **3** is made of dinuclear [Ni$_2$(μ-pmtz)(tren)$_2$]$^{3+}$ units and three perchlorate anions (Figure 4). Within the dinuclear units, the pmtz ligand links two Ni(II) ions with an almost symmetrical k^2N$_1$,N$_7$:k^2N$_4$,N$_{11}$ bis(chelating)/bridging mode. The Ni$^{\mathrm{II}}$ ions exhibit a MN$_6$ distorted octahedral coordination environment, which is made from two *cis* nitrogen atoms belonging to a pmtz ligand (one belonging to the pyrimidine ring and the other one to the tetrazolate ring) and four nitrogen atoms belonging to the tren ligand. Ni−N distances are in the range 2.056(6)−2.203(5) Å, the longer ones being those involving the nitrogen atoms of the pmtz ligands. The distortion of the NiN$_6$ octahedron is mainly due, as in **1**, to the small bite of the pmtz ligand with N$_{\mathrm{pym}}$−Ni−N$_{\mathrm{tetr}}$ angles of about 78°. There exist hydrogen bond interactions in the structure involving the N1B and N7B nitrogen atoms of the tren ligand and the O5 oxygen atom belonging to a perchlorate anion with O5···N1 and O5···N7 distances of 2.974 Å and 2.978 Å, respectively. Likewise,

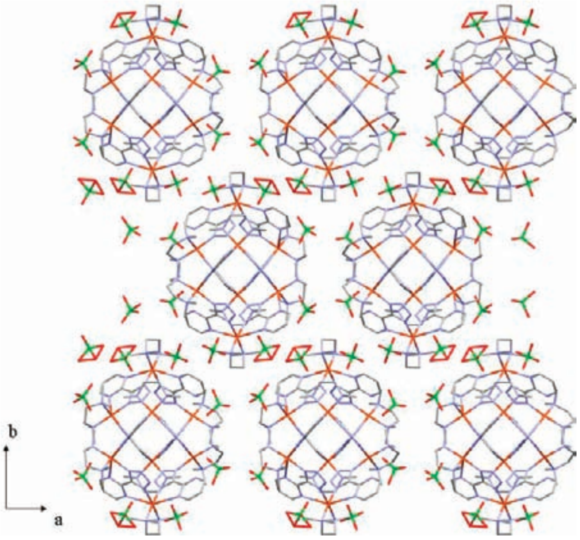

Figure 2. View of the packing of **1** down the *c* axis. H-atoms are omitted for the sake of clarity.

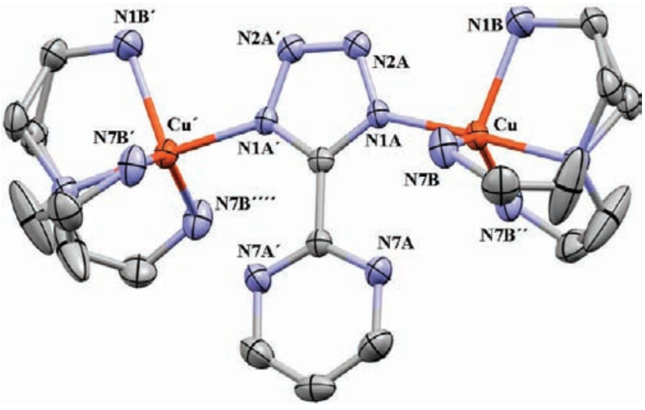

Figure 3. Perspective view of the of the structure of **2**. Perchlorate anions and H-atoms are omitted for the sake of clarity.

neighboring dinuclear units are connected by hydrogen bonds involving the N3A tetrazolate nitrogen atom and the N10C atom belonging to the tren ligand, with a N···O distance of 2.987 Å. The intradinuclear Ni···Ni distance is 5.680 Å whereas the shortest interdinuclear Ni···Ni distance is 7.038 Å.

The structure of **4** consists of pmtz-bridged $\{[Ni_2(pmtz)_2(ampa)_2]^{2+}\}_n$ cationic chains and SCN^- anions (Figure 5). Within the chain, the pmtz ligand links Ni(II) ions in a $k^2N_1,N_7{:}kN_3$ chelating/bridging mode, which is analogous to that found in the two-dimensional (2D) complexes $[M(pmtz)_2]$ (M = Co(II) and Fe(II)).[2a] There are two crystallographically independent Ni(II) atoms in the structure that exhibit a distorted octahedral NiN_6 coordination geometry, the small bite of the pmtz ligand (77.27(18) and 76.83(19)°) being the main cause for such a distortion. Because the three nitrogen donor atoms of the ampa ligand adopt a *mer* conformation on the Ni(II) coordination sphere, the N1 and N7 nitrogen atoms of the chelating part of the pmtz ligand and the N3 atom of a neighboring pmtz ligands are forced to adopt also the *mer* disposition. The N−Ni distances are in the range 2.080(5)−2.183(5) Å, the longer ones corresponding to the N_{pym} and the N_{tetr} bonded to the neighboring Ni(II) ion along the chain. The bridging angles Ni−N1−N2 and N2−N3−Ni are rather asymmetric with values of 137.9(4)° and 139.3(4)° for the former and 121.1(4)° and 123.1(4)° for the latter. The Ni···Ni distances along the chain are 6.203 Å and 6.223 Å, whereas the shortest Ni···Ni interchain distances are 8.376 Å. One of the two crystallographically independent thiocyanate anions is hydrogen-bonded to one of the amino groups of one of the crystallographically independent ampa ligands with a donor-aceptor distance of 3.069(5) Å.

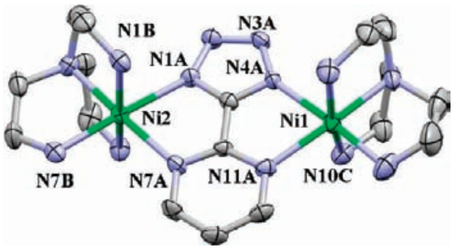

Figure 4. Perspective view of the of the structure of **3**. Thermal ellipsoids are drawn at the 35% probability level. Perchlorate anions and H-atoms are omitted for the sake of clarity.

Magnetic Properties. The temperature dependences of the $\chi_M T$ (χ_M is the molar magnetic susceptibility per Cu_4 unit for **1**, per dinuclear unit for **2** and **3** and per Ni(II) atom for **4**) in an applied magnetic field of 0.5 T for complexes **1**−**4** are shown in Figure 6. At room temperature the $\chi_M T$ values agree well with those expected for four and two non-interacting Cu(II) ions in **1** and **2**, respectively, and two and one non-interacting Ni(II) ions in **3** and **4**, respectively. The χ_M curves (Supporting Information, Figure S1) increase as the temperature is lowered to reach maxima at 17 K, 28 K, 6 and 14 K for **1**−**4**, respectively, and then they decrease at lower temperatures. The occurrence of these maxima in χ_M is characteristic of weak AF coupling between the magnetic ions through the pmtz ligand. For **1**, **2**, and **4**, a low temperature tail is observed, which is due to the presence of a small amount of mononuclear impurity. In keeping with the existence of AF coupling leading to a $S = 0$ ground state, the $\chi_M T$ curves exhibit a slight decrease from room temperature to 50 K for **1** and **3** and to 100 K for **2** and **4**, and then a sharp decrease down to 2 K.

As shown in the crystallographic part, complex **1** is made of Cu_4 entities, where the pmtz ligand acts with a bis(chelating)/bridging mode affording a quasi-square system. Although the Cu···Cu distances and bond angles in the bridging regions are not equal they are very close. In view of this, the magnetic properties of **1** were analyzed by using the following isotropic Hamiltonian with $S = 1/2$, where all the side copper−copper magnetic couplings were considered identical and therefore exhibiting a single *J* value (see Scheme 2).

$$H = -J(\hat{S}_1\hat{S}_2 + \hat{S}_2\hat{S}_3 + \hat{S}_3\hat{S}_4 + \hat{S}_4\hat{S}_1) - j(\hat{S}_1\hat{S}_3 + \hat{S}_2\hat{S}_4)$$

Because the *j* parameter is expected to be very small compared to *J* and to avoid the presence of too many adjustable parameters, the *j* parameter was considered to be negligible. A parameter (*P*) was included to account for the mononuclear impurity. Simulation of the magnetic

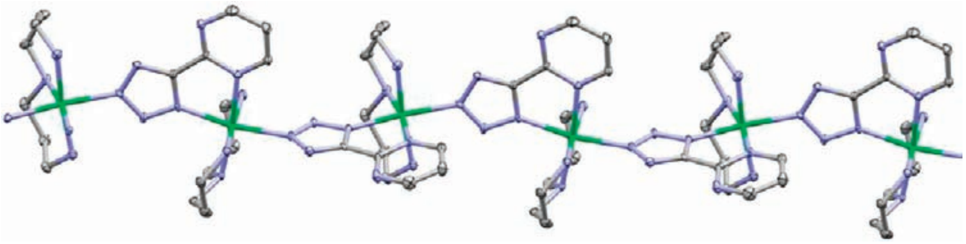

Figure 5. View of the of the structure of **4**. Thermal ellipsoids are drawn at the 50% probability level H-atoms are omitted for the sake of clarity. Nickel(II), nitrogen and carbon atoms are green, blue and gray, respectively.

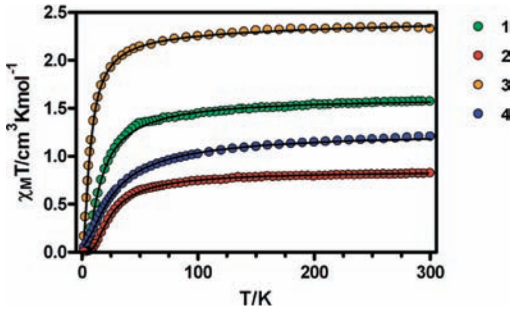

Figure 6. Temperature dependence of $\chi_M T$ for compounds **1**−**4**.

Scheme 2. Magnetic Exchange Pathways in **1**

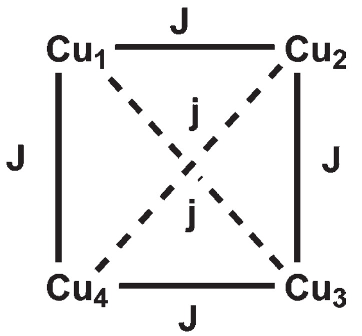

susceptibility data using the MAGMUN program[14] led to $J = -14.1(1)$ cm^{-1}, $g = 2.076(2)$, and $P = 0.018(2)$. The magnetic exchange coupling for **1** is weaker than those observed for polynuclear copper(II) complexes with bis(chelating)/bridging pyrimidine ligands that connect equatorial positions of planar, square-based pyramidal or 4 + 2 tetragonally elongated distorted octahedral copper(II) ions, with $-J$ values in the range 139−238 cm^{-1}. The J value for **1** is even lower than those found for dinuclear copper(II) complexes where only one Cu-pyrimidine-Cu pathway is operative.[15]

The magnetic data of **2** and **3** were fitted to the theoretical equation derived from the isotropic Hamiltonian: $H = -J\hat{S}_1\hat{S}_2$. The best fit parameters were $g = 2.135(3)$, $J = -31.1(1)$ cm^{-1}, and $P = 0.007(2)$ for **2**, and $g = 2.123(3)$ and $J = -4.09(1)$ cm^{-1} for **3**. It should be noted that the J value for **3** is about a quarter of those observed for the analogous bipyrimidine-bridged Ni(II) dinuclear complexes bearing *N*-coordinated peripheral ligands with J values between −16.8 cm^{-1} and −18.3 cm^{-1}.[16]

Since the two Ni···Ni distances along the chain in **4** are very close (6.203 and 6.223 Å), the susceptibility data were fitted using the equation derived by Weng[17] from ring chain calculations for an AF chain of equally spaced $S = 1$ ions, on the basis of the isotropic Hamiltonian $H = -J\sum_i\hat{S}_i\hat{S}_{i+1}$. A parameter ($P$) was included to account for the mononuclear impurity. The best fitted parameters were: $J = -8.7(1)$ cm^{-1}, $g = 2.181(1)$, and $P = 0.0117(1)$. As expected, the fit of the magnetic data to the analytical expression for an AF/AF alternating chain system[18] with local spins $S = 1$ derived from the spin Hamiltonian $H = -J_1[\sum_{i=1}^{N}\hat{S}_{2i}\hat{S}_{2i+1} + \alpha\sum_{i=1}^{N}\hat{S}_{2i}\hat{S}_{2i-1}]$, where $\alpha = J_2/J_1$, led to $\alpha = 1$ and J_1 and g values that, between the experimental errors, are virtually identical to those found for the non-alternating model. It should be noted that for α values close to 1 and $D/|J_1|$ values lesser than 1, as in this case (the absolute D values for isolated Ni(II) centers are commonly found in the range 2−4 cm^{-1}), the influence of local anisotropy will remain a weak effect, very difficult to evidence from the magnetic susceptibility data.[18] This is the reason why we have not considered the influence of the local anisotropy in the Hamiltonian used for analyzing the magnetic data of **4**.

From the above structural and magnetic data, the following assumptions can be drawn:

(1) The magnetic exchange coupling transmitted by the bis(chelating)/bridging pmtz ligand is of much lower magnitude than that mediated by the bipyrimidine analogue bridging mode, all other factors being constant.
(2) The value of Cu−N−C bridging angles in the imidazolyl bridging mode significantly affects the magnitude of the magnetic exchange coupling. Thus, the greater the Cu−N−C angle, the stronger is the AF interaction.
(3) The tridentate chelating/bridging mode is more effective in mediating AF exchange interactions than the bis(chelating)/bridging one.

To theoretically support the above assumptions, DFT calculations were performed on the X-ray structures as well as on model compounds.

---

(14) *MAGMUN*, 4.0/OW0L is available as a combined package free of charge from the authors at http://www.ucs.mun.ca/lthomp/. MAGMUN was developed by Xu, Z.; Thompson, L. K. (Memorial University), and OW01.exe by Waldmann, O. (University of Bern). The software calculates the total spin state values (S) and their associated energies (E) using the Kambe approach, and then substitutes the S and E values into the van Vleck equation to generate the variable-temperature susceptibility profile (degenerate states are accounted for).

(15) Suárez-Varela, J.; Mota, A. J.; Aouryaghal, H.; Cano, J.; Rodríguez-Diéguez, A.; Luneau, D.; Colacio, E. *Inorg. Chem.* **2008**, *47*, 8143.

(16) Suárez-Varela, J.; Sakiyama, H.; Cano, J.; Colacio, E. *Dalton Trans.* **2007**, 249 and references therein.

(17) Weng, C. Y. Ph.D. Thesis, Carnegie Institute of Technology, Pittsburgh, PA, 1968.

(18) Borrás-Almenar, J. J.; Coronado, E.; Curely, J.; Georges, R. *Inorg. Chem.* **1995**, *34*, 2699.

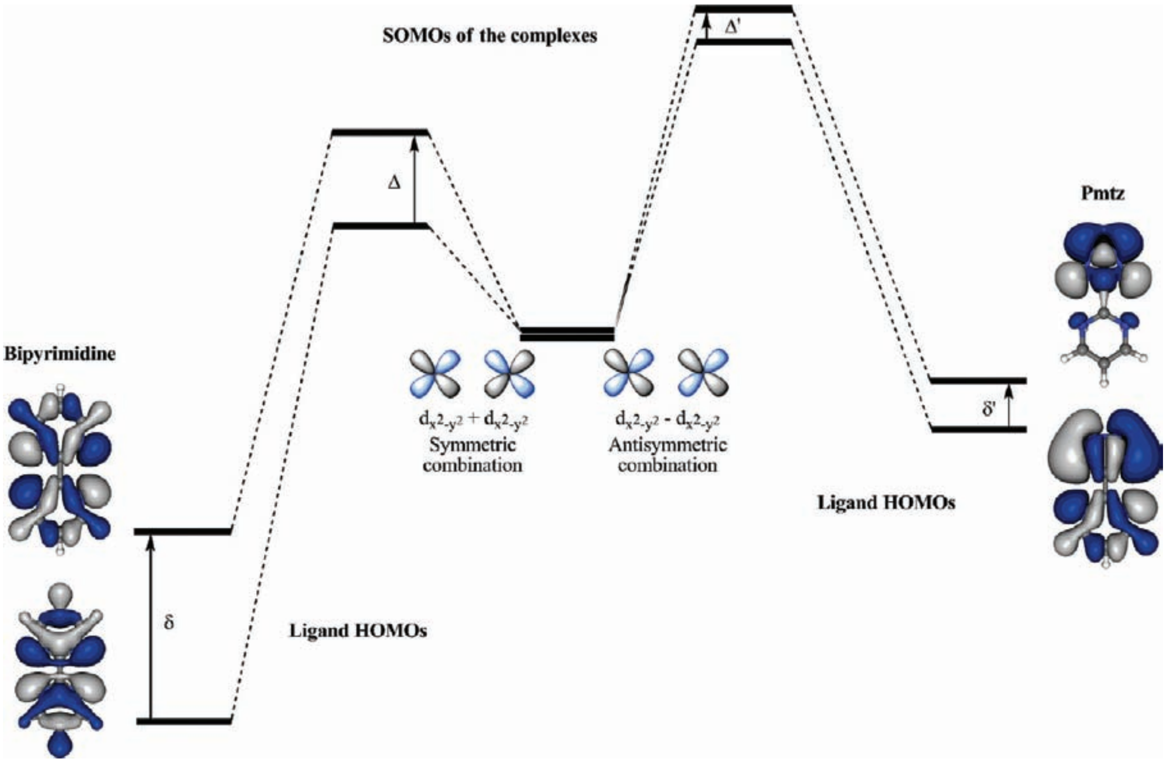

Figure 7. Qualitative diagram of the building of SOMOs from the bipyrimidine and pmtz ligand orbitals. Δ and δ represent the energy gaps between the SOMOs and ligand orbitals involved in the SOMOs formation, respectively.

It should be noted, with regard to point 1, that the most important factor affecting the magnitude of the energy gap between the SOMOs (single-occupied molecular orbitals) in a dinuclear complex (Δ) is the gap between the ligand molecular orbitals involved in the SOMOs formation (δ): the larger the δ value, the bigger is the value of Δ (see Figure 7). The value of δ for the pmtz ligand is much smaller than that for the bipyrimidine ligand (2324 cm^{-1} vs 14457 cm^{-1}) and, consequently, a smaller Δ value is expected for pmtz-bridged dinuclear complexes. Because the AF magnetic contribution to the magnetic exchange coupling depends on Δ,[19] a smaller AF interaction would be expected for pmtz bridged-complexes in accordance with the experimental results.

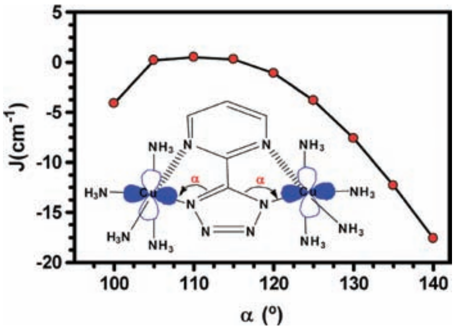

Figure 8. Calculated magnetic coupling constants, J, for the model compound given in the inset viewed in perspective, as a function of the Cu$-$N$_{\text{tetr}}$$-$C angle α.

As indicated above, copper atoms in **1** exhibit a 4 + 2 tetragonally elongated octahedral coordination, with the $d_{x^2-y^2}$ magnetic orbital directed toward the N$_{\text{tetr}}$ and N$_{\text{tmda}}$ nitrogen atoms. The magnetic exchange interactions through the pyrimidine part of the pmtz ligand can be considered as negligible because the N$_{\text{pym}}$ atoms are semicoordinated in axial positions with N$_{\text{pym}}$$-$Cu distances of about 2.7 Å. Therefore, the imidazolyl exchange pathways are the only responsible ones for the magnetic coupling observed in **1** (J = $-$14.1 cm^{-1}). The J values calculated from the X-ray crystal structure of **1** show three almost equal exchange pathways (two J = $-$6.3 cm^{-1} and one J = $-$6.0 cm^{-1}), whereas the other one mediates a weaker magnetic coupling characterized by a J = $-$2.7 cm^{-1} (see Supporting Information, Figure S1). The smaller J value corresponds to the imidazolyl exchange pathway that exhibits the smaller Cu$-$C$-$N$_{\text{tetr}}$ angles. In view of these results, it seems that the AF coupling increases with the increase of the C$-$N$_{\text{tetr}}$$-$Cu angle. To support this hypothesis (point 2) we have performed DFT calculations on a model consisting of a symmetrical dinuclear fragment in which each tmda ligand, and the N$_{\text{tetr}}$ and the N$_{\text{pym}}$ nitrogen atoms of the neighboring pmtz ligands, have been substituted by ammonia molecules with a fixed N$-$Cu distance of 2.0 Å (Figure 8). In this model, the $d_{x^2-y^2}$ magnetic orbital lies in a plane almost perpendicular to the pmtz plane. The J values were calculated by varying the α angles in the 100$-$140° range. For α = 120°, the calculated J value was found to be $-$1.1 cm^{-1}, which is very close to the value of $-$2.7 cm^{-1} calculated for the fragment in the tetranuclear unit of **1** having the smaller α values. These results demonstrate the suitability of the model. As it can be observed in Figure 8, the AF coupling decreases with the decrease of α from $-$17.6 cm^{-1} at 140° to $-$1.1 cm^{-1} at 120°. From this later angle to 105°, the

---

[19] (a) Hay, P. J.; Thiebault, J. C.; Hoffmann, R. *J. Am. Chem. Soc.* **1975**, *97*, 4884. (b) Kahn, O.; Briat, B. *J. Chem. Soc., Faraday Trans. 2* **1976**, *72*, 268.

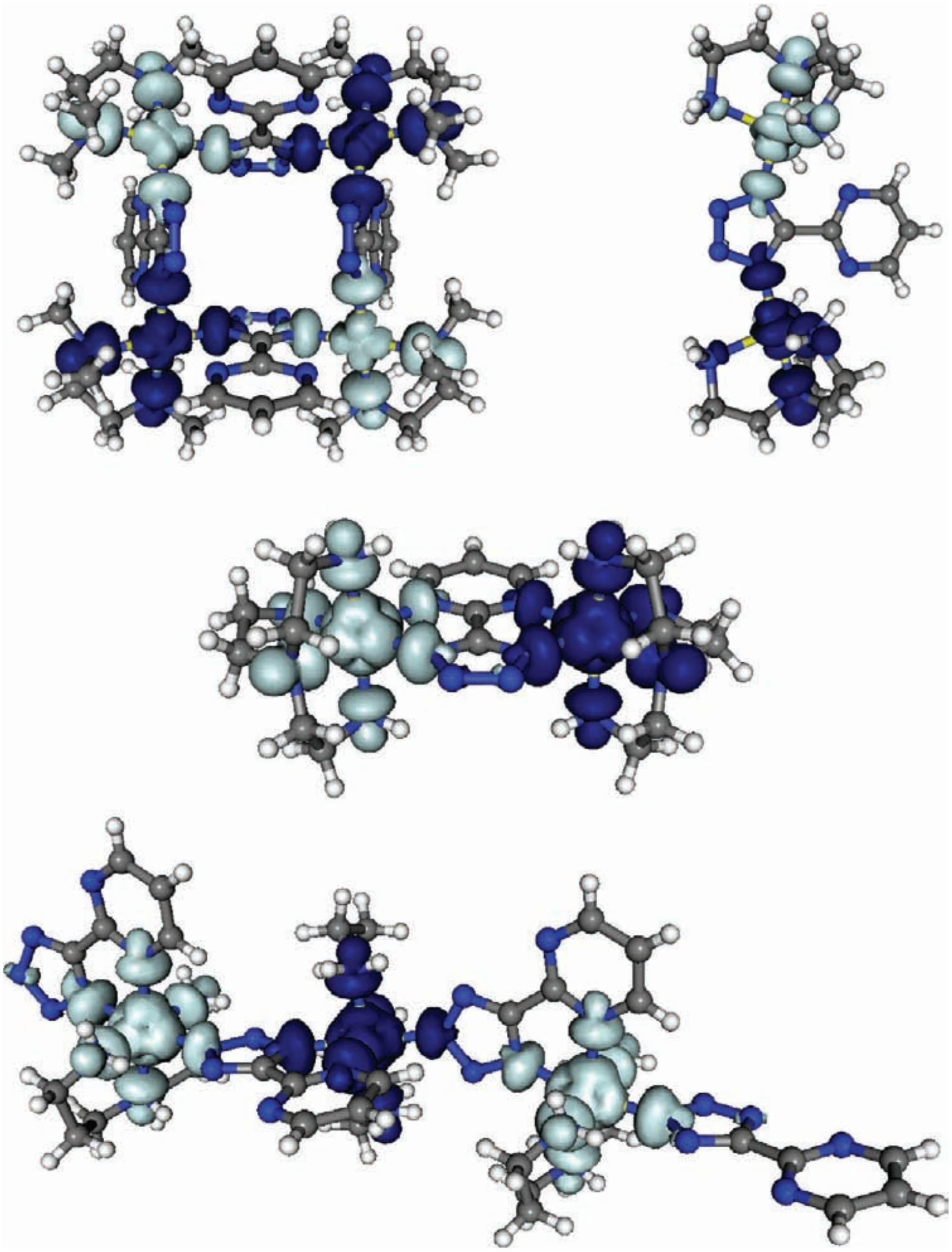

Figure 9. Calculated spin density distribution for the broken-symmetry singlet states of **1** (top left), **2** (top right), **3** (middle), and the trinuclear fragment of **4** (down). Positive and negative values are represented as gray and blue surfaces, respectively. The isodensity surfaces represented correspond to cutoff values of 0.0020 (**1** and **2**), 0.0013 (**3**), and 0.0016 (**4**) e bohr^{-3}.

interaction becomes very weakly ferromagnetic, and below 105° the interaction becomes again AF.

The magneto-structural data for **2** confirm this trend. This compound has a Cu$-$N$_{tetr}-$C angle (α = 130.5°) bigger than those found in **1** (average value of 122°) and therefore a stronger AF coupling is observed ($J = -14.1$ cm^{-1} for **1** and $J = -31.1$ cm^{-1} for **2**). The calculated J value for **2** of -14.2 cm^{-1} is also in good accord with the theoretical tendency shown in Figure 8. Because other structural factors, such as a distortion of the equatorial copper(II) coordination plane, the shift of the copper(II) atoms from the pyrimidine ring of the pmtz ligand, the copper(II)$-$copper(II) distance, and so forth, can also affect the strength of the AF coupling, the theoretical dependence of J with the Cu$-$N$_{tetr}-$C angle given in Figure 8 is nothing more than a qualitative trend with a relatively accurate predictive value. It should be noted at this point that the substitution in the model with α = 120° of the pyrimidine ring by a hydrogen atom or by a carboxylate group does not change significantly the magnetic coupling, showing in both cases a J value of -1.5 cm^{-1}.

Despite the good qualitative agreement in sign and magnitude order between theoretical and experimental results for compounds **1** and **2**, the J values obtained by DFT calculations are almost half of the experimental ones, as reported by ourselves for other copper polynuclear complexes.[20] This may be due to either intrinsic

---

(20) Palacios, M. A.; Rodríguez-Diéguez, A.; Sironi, A.; Herrera, J. M.; Mota, A. J.; Cano, J.; Colacio, E. *Dalton Trans.* **2009**, 8538.

Table 2. Spin Densities and J Values for **1−5**

	1	**2**	**3**	**4**^{j}	**5**	**6**	**7**	**8**
$J_{\mathrm{exp}}{}^{a}$	$-14.1(1)$	$-31.1(1)$	$-4.09(1)$	$-8.7(1)$	$-^{b}$	$-^{b}$	$-^{b}$	$-^{b}$
$J_{\mathrm{calc}}{}^{a}$	$J_1{}^{c} = -6.0$ $J_2 = J_3 = -6.3$ $J_4 = -2.7$	-14.2	-2.9	$J_1{}^{d} = -6.8$ $J_2 = -7.2$	-16.9^{e}	-51.5	$+55.2$	$+1.3^{k}$
$\sigma_{\mathrm{M1}}{}^{f}$	$+0.5940$	$+0.6421$	$+1.6313$	$+1.6544$	$+0.5629$	$+0.5799$	$+0.5308$	$+0.5830$
σ_{M2}	-0.5924	-0.6409	-1.6243	-1.6582	-0.5629	-0.5672	$+0.5308$	$+0.5830$
σ_{Cu3}	$+0.5909$	$-^{b}$	$-^{b}$	$-^{b}$	$-^{b}$	$-^{b}$	$-^{b}$	$-^{b}$
σ_{Cu4}	-0.5927	$-^{b}$	$-^{b}$	$-^{b}$	$-^{b}$	$-^{b}$	$-^{b}$	$-^{b}$
σ_{Ni3}	$-^{b}$	$-^{b}$	$-^{b}$	$+1.6562$	$-^{b}$	$-^{b}$	$-^{b}$	$-^{b}$
$\sigma_{\mathrm{N1}}{}^{g}$	$+0.0697^{h}$	$+0.0805$	$+0.0429$	$+0.0543^{h}$ -0.0523^{i}	$+0.0879^{h}$	-0.0767	$-^{b}$ $-^{b}$	$-^{b}$ $-^{b}$
σ_{N4}	-0.0697^{h}	-0.0800	-0.0446		-0.0879^{h}	$-^{b}$	$-^{b}$	$-^{b}$
σ_{N7}	$< \|0.0002\|^{h}$	$< \|0.0001\|$	$+0.0267$	$+0.0452^{h}$ -0.0461^{i}	-0.0675^{h}	-0.1007	$-^{b}$ $-^{b}$	$-^{b}$ $-^{b}$
σ_{N11}	$< \|0.0002\|^{h}$	$< \|0.0001\|$	-0.0271		$+0.0675^{h}$	$-^{b}$	$-^{b}$	$-^{b}$
σ_{N2}	$-^{b}$	$-^{b}$	$-^{b}$	$-^{b}$	$-^{b}$	$-^{b}$	$+0.0927$	$+0.0779$
σ_{N3}	$-^{b}$	$-^{b}$	$-^{b}$	$+0.0491^{h}$	$-^{b}$	$+0.0764$	$+0.0927$	$+0.0779$

[a] In cm^{-1}. [b] Not available. [c] See Supporting Information, Figure S1. [d] See Supporting Information, Figure S1. [e] For an α value of 100°. [f] Mulliken spin densities where M = Cu (complexes **1**, **2**, and **5**), Ni (complexes **3** and **4**). [g] Referred to the corresponding nitrogen atoms of the pmtz ligand belonging to the metal coordination sphere. [h] Average values. [i] Values for the central unit. [j] The calculated values were obtained from a model consisting in a trinuclear fragment of the chain of **4**. [k] For $\beta = 130°$ and $\gamma = 100°$, see Figure 10.

limitations of the method and/or to the flexibility exhibited by the structures of **1** and **2**. This flexibility might allow structural changes when the sample is cooled. If these geometrical modifications are not negligible, they can lead to a change in the magnitude of the exchange coupling constant.

As expected, the spin density distributions for the singlet ground states in **1** and **2** (Figure 9) show the predominance of the delocalization mechanism through a σ type exchange pathway involving the $d_{x^2-y^2}$ magnetic orbitals of the copper(II) atoms (in the case of **2** the magnetic orbitals are of the d_{z^2} type) and the sp^2 hybrid orbitals of the tetrazolate nitrogen bridging atoms. For **1**, the spin densities delocalized over the nitrogen bridging atoms are around 0.13 e, and the average spin population on the copper(II) atoms is 0.59 e (see Table 2).

For **2**, the spin density delocalized on the nitrogen atoms of the bridging region is small (0.08 e) and, therefore, the spin density is mainly found at the metal (average value of 0.64 e).

To know how efficient the bis(chelating)/bridging mode is in mediating the magnetic coupling, we have used the model compound $[Cu_2(NH_3)_4(\mu\text{-pmtz})]^+$ (**5**) where the copper(II) ions exhibit a square-planar geometry. The whole compound is planar (the $d_{x^2-y^2}$ magnetic orbital is coplanar with the pmtz ligand), the α angle is 100°, and the $Cu-N_{\mathrm{tetr}}$ and $Cu-N_{\mathrm{pym}}$ bond distances are 2.000 and 1.957 Å, respectively. The calculated J value for this model (-16.9 cm^{-1}) is even larger than that calculated for **2**, thus suggesting that the pyrimidine exchange pathway is also active in the transmission of the magnetic exchange coupling. In keeping with this, the analysis of the spin density distribution (Figure 10) shows that the spin density is delocalized over both the bridging nitrogen atoms of the tetrazolate and pyrimidine rings (see Table 2). Nevertheless, the fact that the spin density is higher for the former than for the bridging nitrogen atoms in the latter (0.08 e vs 0.065 e) might indicate that the tetrazolate pathway is more effective than the pyrimidine one in mediating the magnetic exchange coupling in pmtz-bridged systems. It would have been of interest for comparative purpose to dispose of the magnetic and structural data of a similar bischelating/bridged pmtz dinuclear copper(II) complex, but, unfortunately, we have not been able to obtain suitable crystals of the compound $[Cu_2(\mu\text{-pmtz})(tmda)_2](ClO_4)_2$. Nevertheless, the calculated J value for **3** (a bis(chelating)/bridged pmtz dinuclear Ni(II) complex) is close to that obtained from the experimental magnetic data (-2.9 cm^{-1} vs -4.09 cm^{-1}). As in the model compound $[Cu_2(NH_3)_4(\mu\text{-pmtz})]^+$, the corresponding spin densities (Figure 9 and Table 2) delocalized over the bridging nitrogen atoms of the tetrazolate ring (average value 0.044 e) are higher than those over the bridging nitrogen atoms of the pyrimidine ring (average value 0.027 e). As expected, the spin density is mainly found at the nickel(II) ions (average value of 1.628 e).

To theoretically support the magnetic exchange coupling observed for **4** and consequently the assumption 3, we have calculated the J values for a model compound consisting of a trinuclear fragment of the alternating chain of **4** (see Figure 9). DFT calculations predict moderate AF interactions with $J_1 = -6.8$ cm^{-1} and $J_2 = -7.2$ cm^{-1} for the pmtz pathways with Ni−Ni distances of 6.203 Å and 6.223 Å, respectively. These values agree rather well with the average J value calculated from the fitting of the experimental magnetic susceptibility data of -8.7 cm^{-1}. These results point out that the tridentate chelating/bridging mode is more effective in mediating AF exchange interactions than the bis(chelating)/bridging or imidazoyl/bridging modes. As expected, most of the spin density (see Figure 9 and Table 2) remains on the nickel(II) atoms (average value of 1.65 e), and the spin density delocalized over the pmtz ligand is mainly found on the N1, N7 (average values of |0.0495| e), and N3 (+0.0491 e) nitrogen bridging atoms.

Even though we have not succeeded in obtaining any pmtz-bridged copper complex where the pmtz ligand acts in a tridentate $k^2N_1,N_7{:}kN_3$ chelating/bridging mode, we have calculated the magnetic exchange coupling on the model compound $[Cu(NH_3)_2(\mu\text{-pmtz})Cu(NH_3)_3]^{3+}$ **6** (see Figure 10). The calculated J value of -51.2 cm^{-1} supports that the $k^2N_1,N_7{:}kN_3$ chelating/bridging mode is more effective in transmitting the AF interaction than the bis(chelating)/bridging or imidazolyl/bridging modes in pmtz-bridged complexes.

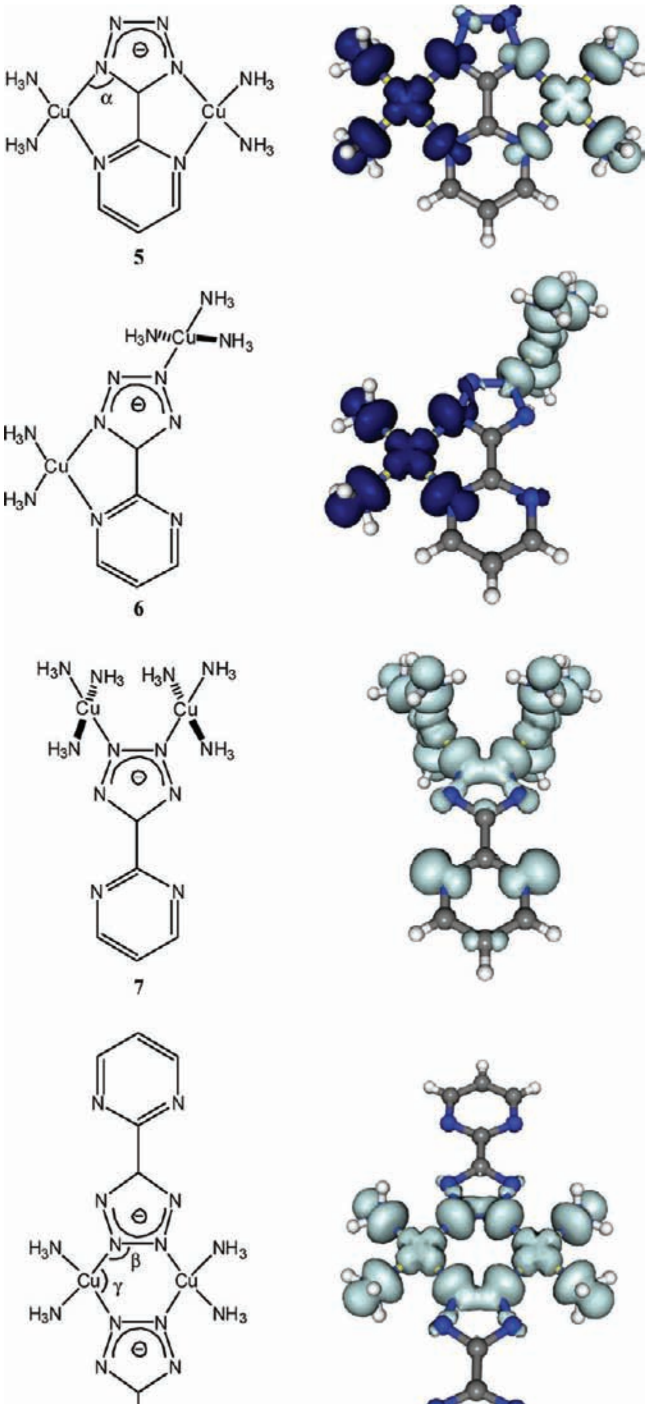

Figure 10. Schematic representations of the model compounds [Cu(NH_3)$_2$(μ-pmtz)Cu(NH_3)$_2$]$^{3+}$ (**5**), [Cu(NH_3)$_2$(μ-pmtz)Cu(NH_3)$_3$]$^{3+}$ (**6**), [Cu(NH_3)$_3$(μ-pmtz) Cu(NH_3)$_3$]$^{3+}$ (**7**), and [Cu(NH_3)$_2$(μ-pmtz)$_2$Cu(NH_3)$_2$]$^{2+}$ (**8**), along with the corresponding calculated spin densities for the broken-symmetry singlet (**5** and **6**) and triplet (**7** and **8**) states. Positive and negative values are represented as gray and blue surfaces, respectively. The isodensity surfaces represented correspond to cutoff values of 0.0013 (**5**, **7** and **8**) and 0.0016 (**6**) e bohr^{-3}.

Finally, to cover the major number of potential simple bridging groups, we have considered another dinuclear model, namely, [Cu(NH_3)$_3$(μ-pmtz) Cu(NH_3)$_3$]$^{3+}$ (**7**) (see Figure 10), where the pmtz ligand adopts an exobidentate kN$_2$:kN$_3$ bridging coordination mode that was previously observed in the dinuclear complex [{Co_2(tren)(μ-pmtz)(μ-O_2)}](ClO_4)$_3$·$3H_2O$.[4b] Thus, for **7**, a moderate ferromagnetic coupling constant of +64.0 cm^{-1} has been calculated (see Table 2). However, on considering the hypothetical dimer of **7** [Cu(NH_3)$_2$(μ-pmtz)$_2$Cu(NH_3)$_2$]$^{2+}$ (**8**), it has been demonstrated that this coordination mode could exhibit either antiferro- or ferromagnetic behavior depending on geometric parameters as angles β and γ (see Figure 10). Therefore, for $\beta = \gamma = 120°$, a very weak AF interaction is calculated ($J = -4.0$ cm^{-1}). When the γ angle is gradually closed, with the concomitant opening of the β angle, the AF decreases and even ferromagnetic interactions can be obtained. For $\gamma = 100°$ and $\beta = 130°$, however, $J = +1.3$ cm^{-1} whereas for $\gamma = 80°$ and $\beta = 140°$, $J = +16.0$ cm^{-1}.

Concluding Remarks

The versatile ligand pmtz, with six basic nitrogen atoms, reacts with Cu(II) and Ni(II) ions in the presence of bi- and tridentate amines to afford pmtz-bridged complexes. Depending on the stereoelectronic preferences of the metal ion and the coordination properties of the polyamine (denticity and relative disposition of the donor atoms), complexes exhibiting different pmtz-bridging coordination modes were obtained: (i) asymmetric k^2N$_1$,N$_7$:k^2N$_4$,N$_{11}$ bis(chelating)/bridging mode for the tetranuclear complex [Cu_4(μ-pmtz)$_4$(tmda)$_4$](ClO_4)$_4$ (**1**), (ii) a novel symmetric kN$_1$:kN$_4$ imidazolyl bridging mode for the dinuclear complex [Cu_2(μ-pmtz)(tren)$_2$](ClO_4)$_3$ (**2**), (iii) symmetric k^2N$_1$,N$_7$:k^2N$_4$,N$_{11}$ bis(chelating)/bridging mode for [Ni_2(μ-pmtz)(tren)$_2$](ClO_4)$_3$ (**3**), and (iv) tridentate k^2N$_1$,N$_7$:kN$_3$ chelating/bridging mode for the chain complex [Ni_2(μ-pmtz)$_2$(ampa)$_2$]$_n$(SCN)$_{2n}$ (**4**). If the long distances of the Jahn−Teller 4 + 2 tetragonally distorted Cu(II) ions in **1** are considered as non-bonding distances, the pmtz ligand exhibits, as in **2**, k-N$_1$:k-N$_4$ imidazolyl bridging mode. These results suggest that the coordination of the pmtz ligand to a CuL moiety in a monodentate form through the N1 tetrazole nitrogen atom may induce the binding of the second CuL unit to the N4 tetrazole nitrogen atom, giving rise to an imidazolyl bridging mode, as observed for **1** and **2**. Moreover, it seems that the symmetric N1, N7 chelating coordination of the pmtz ligand (only observed for the Ni(II) ions that show a great tendency to adopt an octahedral coordination geometry) may lead to either bis(chelating)/bridging or tridentate/bridging coordination modes as observed in **3** and **4**, respectively.

The compounds exhibit weak to medium AF interactions via the pmtz bridging ligand. DFT calculations have demonstrated that this is mainly due to the small gap between the pmtz molecular orbitals involved in the SOMOs formation. The magneto-structural data for compounds **1** and **2** show that the magnitude of the AF interaction observed for imidazolyl pmtz-bridged complexes depends on the Cu−N−C angle, so the AF interactions increase as the angle goes up. This experimental result has been supported by theoretical calculations on model compounds, which show that the main factor determining the magnetic coupling in imidazolyl pmtz-bridged complexes is the value of the Cu−N−C angle. Experimental results and theoretical calculations demonstrate that the tridentate chelating/bridging mode is more effective in mediating AF exchange interactions than the bis(chelating)/bridging or imidazolyl/bridging modes in pmtz-bridged complexes. Finally, theoretical calculations have shown that ferromagnetic interactions might be obtained for copper(II) complexes bearing N2, N3 pyrazoyl-bridged pmtz ligands with Cu−N2−N3 bridging angles smaller than 100°.

Acknowledgment. This work was supported by the MEC (Spain) (Project CTQ-2008-02269/BQU), the Junta de Andalucía (FQM-195 and Projects of excellence P08-FQM-03705 and P07-FQM-03092) and the University of Granada (grant to A.J.M., J.M.H., and A.R.-D.). M.A.P thanks to the Ministerio de Ciencia e Innovación of Spain for a FPI grant. We would like to thank the Centro de Supercomputación de la Universidad de Granada for computational resources. The authors are also grateful to Dr. Joan Cano, University of Valencia, Spain, for his continuous and generous assistance with the DFT calculations.

Supporting Information Available: Crystallographic data in CIF format, and Figure S1. This material is available free of charge via the Internet at http://pubs.acs.org.